1044 Bull. Chem. Soc. Jpn. Vol. 80, No. 6, 1044–1057 (2007)

Vol. 80 Commemorative Accounts

Synthetic Multifunctional Nanoarchitecture in Lipid Bilayers: Ion Channels, Sensors, and Photosystems†

Rajesh Bhosale, Sheshanath Bhosale,† Guillaume Bollot, Virginie Gorteau, Marc D. Julliard, Svetlana Litvinchuk, Jiri Mareda,* Stefan Matile,* Tomohiro Miyatake, Federico Mora, Alejandro Perez-Velasco, Naomi Sakai,* Adam L. Sisson, Hiroyuki Tanaka, and Duy-Hien Tran

Department of Organic Chemistry, University of Geneva, Geneva, Switzerland

Received February 5, 2007; E-mail: stefan.matile@chiorg.unige.ch

The creation of functional materials such as ion channels, porous sensors, or smart photosystems depends critically on our ability to assemble sophisticated, error-free and self-repairing nanoarchitecture in a predictable manner. To address these challenging topics, we often used lipid bilayer membranes as compartmentalizing platform and have introduced rigid-rod molecules as privileged scaffolds that bypass all folding problems because they do not fold. This approach provides access to motifs such as rigid-rod barrels, helices, stacks, slides, and wires that can act as smart, stimuli-responsive photosystems, pores, ion channels, hosts, sensors, and catalysts. The selected examples focus on naphthalenediimides (NDIs), a compact, organizable, colorizable, and functionalizable n-semiconductor. This versatile module is used in rigid-rod molecules to mediate transmembrane anion transport by anion–π interactions, as sticky π-clamp within pore sensors to catch otherwise elusive analytes by aromatic electron donor–acceptor interactions, or in blue, transmembrane π-stack architecture to collect and convert photonic energy. These specific examples with multifunctional NDI nanoarchitecture are of help to outline, on the one hand, possibilities to contribute to advanced functional materials such as multianalyte sensors or solar cells and, on the other hand, to keep on wondering about an enormous structural and functional space waiting to be explored.

In biology, highest sophistication on both the structural and functional level is accomplished with membrane proteins. Ion channels and pores, for instance, function as stimuli-responsive multianalyte sensors that assure perception of and communication with the outside world.[1–7] The conversion of photonic energy into chemical energy is another essential biological process that takes place in biomembranes.[8–10] Rapidly increasing insights on the molecular structure reveal that these remarkable processes are accomplished by perfect nanoarchitecture of exceptional complexity and beauty.[1–10] The bilayer membrane provides not only a privileged platform for the assembly of such biological multifunctional systems. As a compartmentalizing barrier, it also introduces the directionality that is needed for energy conversion, signal transduction, remote control of chemical processes, and so on.

For the synthetic organic chemist, the bilayer membrane provides an ideal starting point to create from scratch new architecture with, hopefully, new functions rather than to simply use the given, perfect biological architecture. To do so, we have introduced rigid-rod molecules as privileged scaffolds that bypass all folding problems because they do not fold.[11,12] Somehow the antithesis to foldamers,[13,14] these simple sturdy rods have attracted considerable scientific attention for applications in the materials sciences.[15–25] Highlights beyond the minimalist oligoacetylenes[17] **1** and *p*-oligophenyls[18,19] **2** include the oligonaphthalenes **3** studied in the Tsubaki group because of their exceptional stereochemical complexity (Fig. 1).[20] Important for nanoarchitecture, this non-planarity is lost in the flattened rylene rods **4** from the Müllen group.[21] The longer versions of these rods are very interesting because they can harvest infrared light. Eaton's oligocubanes **5** are a spectacular example for a rich collection of non-aromatic and non-planar rigid rods in the literature.[22] Pioneered in the Miller group, rigid oligonaphthalenediimide (O-NDI) rods **6** are of interest because NDIs are one of the few stable organic n-semiconductors.[23] Also of interest in optoelectronics, oligoperylenediimides (O-PDIs) **7** are another example for rigid-rod molecules with atoms other than carbon in their scaffold.[24] The longest monodisperse rigid-rod molecule prepared so far is Osuka's 128-mer of oligoporphyrin **8**: $l = 1060$ Å.[25]

Although molecular rods such as DNA duplexes or α-helices are ubiquitous in biology, rigid rods do not exist. To change this situation and explore the usefulness of rigid-rod molecules to address challenging biological questions of current concern, we originally selected *p*-oligophenyls **2** as model

---

† Present address: School of Chemistry, Monash University, Victoria, Australia

Published on the web June 13, 2007; doi:10.1246/bcsj.80.1044

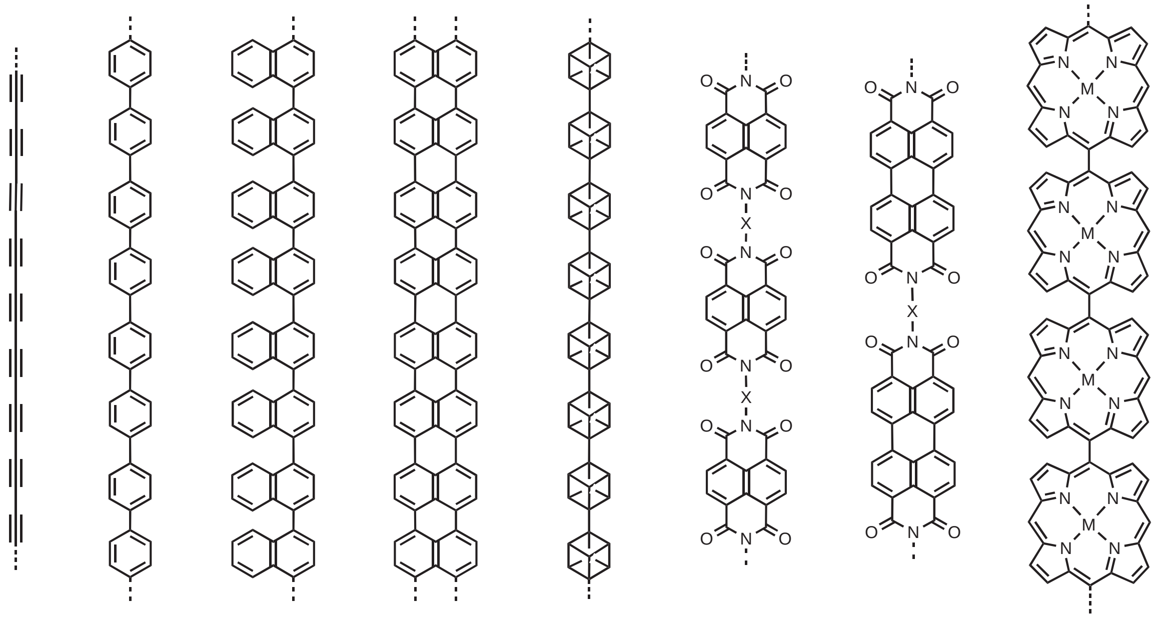

1 2 3 4 5 6 7 8

Fig. 1. Selected rigid-rod molecules, members of a shape-persistent family of molecules that does not fold.

rods.[11,12] This choice was made because *p*-oligophenyls are not only quite easy to synthesize and derivatize, but also because they are non-planar, chiral and fluorescent. Non-planarity, that is the biphenyl torsions in the *p*-oligophenyl scaffold, is essential to control supramolecular architecture. Chirality and fluorescence are helpful for structural studies in more complex systems such as lipid bilayer membranes under conditions that are relevant for significant function, e.g., nanomolar or low micromolar concentrations.

In the following, we first outline the synthesis of multifunctional nanoarchitecture with a representative recent example and provide an overview of the systems studied over the past decade. Then, we zoom in on three recent studies that introduce the π-acidic naphthalenediimide (NDI) as versatile module for the creation of multifunctional nanoarchitecture. The first example with O-NDIs as anion–π slides underscores our interest in synthetic ion channels and pores.[26] The second example with NDI as sticky π-clamps within multifunctional rigid-rod β-barrels describes synthetic pores as sensors.[27] In the third example, colorful, blue, red-emitting NDI π-stacks along transmembrane *p*-oligophenyl scaffolds illustrate recent developments toward artificial photosynthesis and photovoltaics.[28]

Multistep Synthesis of Multifunctional Nanoarchitecture

The ability to create new compounds from scratch will always be the distinguishing expertise of the organic chemist (and will always be needed). This art of organic synthesis is extensively practiced in the research described in the following. The synthesis of photoactive rigid-rod quadruple π-*M*-helix **9**, reported last year, may illustrate this point (Scheme 1).[28] The rigid-rod scaffolds **10** and the blue, red-emitting NDI chromophores **11** were accessible from simple commercially available starting materials such as biphenyl **12** and pyrene **13**, respectively.

Our classical approach to multisubstituted *p*-octiphenyls such as **10** begins with the nucleophilic aromatic substitution with iodide.[11,29] The resulting $1^4,2^4$-diiodobiphenyl **14** was then exposed to *n*-butyllithium and quenched with MeOH to replace one iodide with a hydrogen. The resulting iodobiphenyl **15** was then either converted into boronate **16** or subjected to an oxidative coupling to give diiodo-*p*-quarterphenyl **17**. The same *p*-quarterphenyl **17** could be obtained by Suzuki coupling of iodobiphenyl **15** and boronate **16**.

Regioselective iodination of both termini of *p*-quarterphenyl **17** was possible using the bulky *t*-butyllithium instead of *n*-butyllithium for *p*-oligophenyl deprotonation. Suzuki coupling of the obtained $1^4,4^4$-diiodo-*p*-quarterphenyl **18** with biphenyl diboronate **16** gave with $1^3,2^3,3^2,4^3,5^2,6^3,7^2,8^3$-octakismethoxy-*p*-octiphenyl **19** the desired rigid-rod scaffold. Replacement of the methyl ethers in the poorly soluble **19** with *t*-butyl glycolates resulted in highly soluble product **20**. Mild deprotection with TFA produced the carboxylic acids along the rigid-rod scaffold **10** for reaction with the blue amines **11**.

Following the original Vollmann–Würthner procedure,[30] the synthesis of these chromophores was initiated with the oxidative chlorination of pyrene **13** to dianhydride **21**. Introduction of, first, the amines **22** and **23** produced diimide **24**. Subsequent nucleophilic aromatic substitution with isopropylamines **25** at the π-acidic NDI core gave the desired blue NDI module **26**. Chemoselective alloc removal with Bu_3SnH and $Pd(PPh_3)_2Cl_2$ produced amine **11** for reaction with the carboxylic acids along the rigid-rod scaffold **10**. The obtained NDI *p*-octiphenyl conjugate **27** was deprotected with TFA to give target molecule **28** for the self-assembly of photosystem **9** in lipid bilayer membranes (see below).

This specific example of the multistep synthesis of multifunctional nanoarchitecture is shown to underscore that this research provides appreciable experience in organic synthesis and produces useful compounds. Outstanding functions rou-

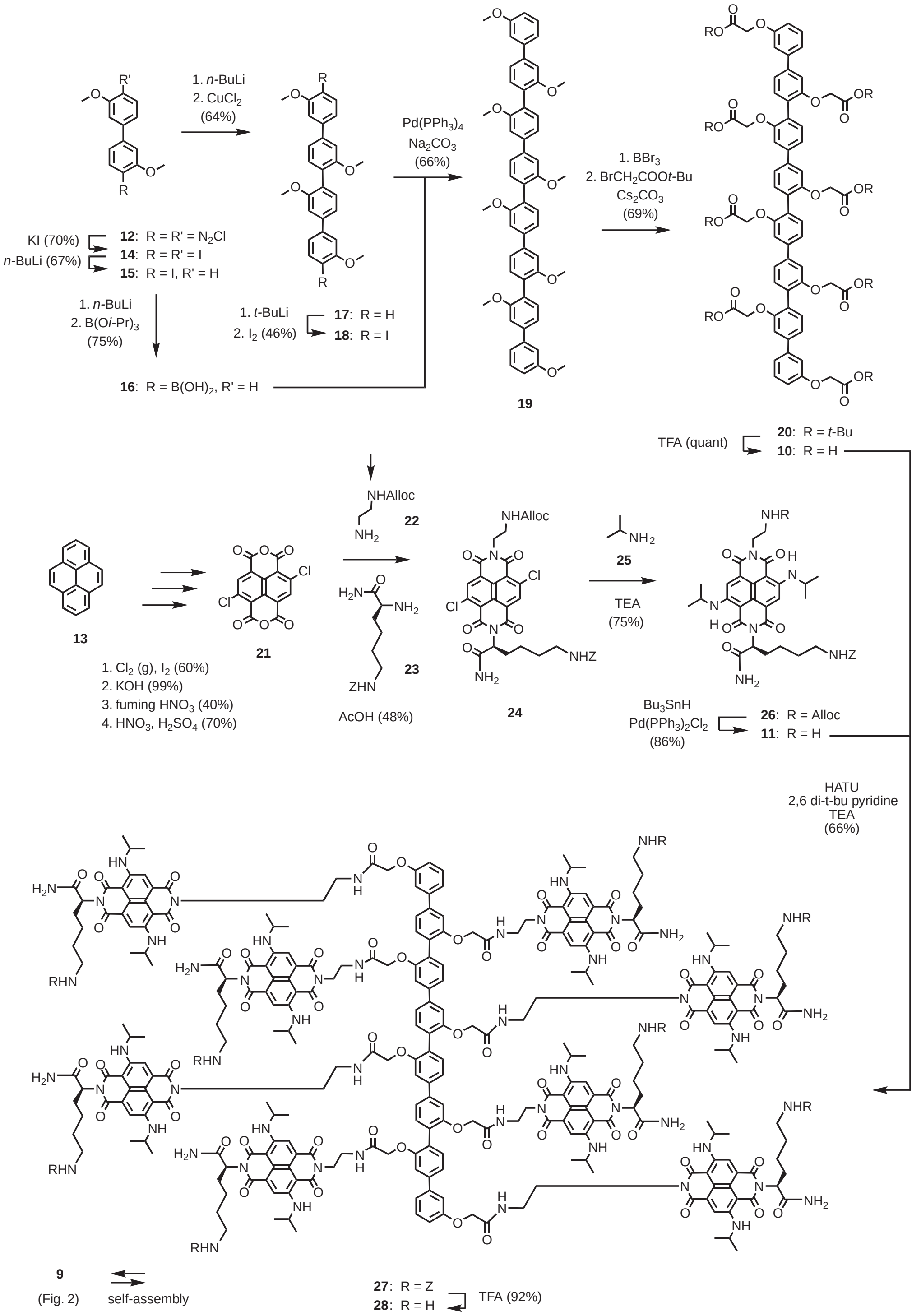

Scheme 1. Synthesis of photosystem **9**.

tinely obtained with advanced rigid-rod nanoarchitecture suggest that these quite substantial synthetic efforts are absolutely worthwhile. Multifunctional rigid-rod nanoarchitecture beyond rigid-rod π-helices **9**[28,31] synthesized so far includes rigid-rod proton wires **29**,[11,32] rigid-rod π-slides **30**,[33] rigid push–pull rods **31**,[34,35] and rigid-rod β-barrels **32** (Fig. 2).[12,36] In proton wire **29**, a hydrogen-bonded chain (HBC) is established along a rigid-rod scaffold that is long enough to span a lipid bilayer.[32] To move now a proton across the membrane, first it has to hydrogen-bond to the terminal oxygen atom of the HBC. Then, by flipping all hydrogen-bond protons, hop along the HBC to liberate the proton from the oxygen atom at the other end of the HBC on the other side of the membrane (Fig. 2a). Then, all C–O bonds turn around to return to the resting state to transport the next proton (Fig. 2b). Rigid-rod proton wire **29** thus represents a functional model of the Onsanger hop-turn mechanism, a mechanism that is thought to play a central role in bioenergetics.

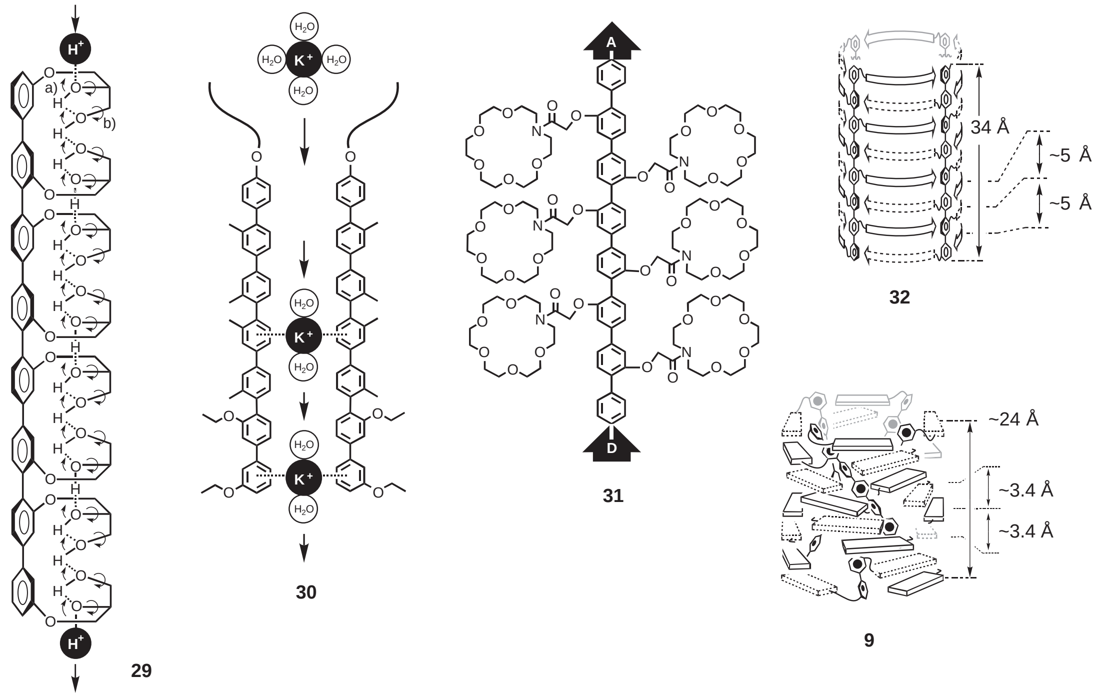

Fig. 2. Functional architecture with rigid *p*-oligophenyl scaffolds synthesized and studied over the past decade includes transmembrane hydrogen-bonded chains **29** for selective proton transport, cation–π slides **30** for selective potassium transport (see Fig. 3), rigid push–pull rods **31** for voltage gating, rigid-rod β-barrels **32** for synthetic multifunctional pores (see Fig. 4–6), and rigid-rod π-helices **9** for artificial photosynthesis (see Fig. 7).

Until recently,[26] cation–π slide **30** was the only example available for rigid-rod scaffolds that do not only play a structural but also a functional role.[33] The concept of cation–π slides motif builds on pioneering work from the Kobuke group, where cation–π interactions within amphiphilic resorcin[4]arenes were envisioned to account for cation selective transport with sequence $K^+ > Na^+ \gg Rb^+$ (blockage).[37] Computational studies from the Dougherty group suggested that loosening up of the fixed distances between the aromatic rings as in resorcin[4]arenes may provide access to the Eisenmann IV selectivity sequence $K^+ > Rb^+ > Cs^+ > Na^+ > Li^+$ found in biological potassium channels.[1,2,38,39] An assembly of *p*-septiphenyls **30** was envisioned to place seven of such flexible, non-covalent arene macrocycles covalently on top of each other across a lipid bilayer. A recognition unit was attached to one end of the *p*-septiphenyls for remote control of rod assembly by chemical stimulation. The π-basicity of benzene rings was expected to allow selective potassium hopping along the dynamic cation–π slides. The found transition from a Eisenmann III to a more pronounced Eisenmann IV selectivity in response to ligand-gated rod assembly was in excellent agreement with these expectations. The complementary anion–π slides[26] will be described in the next chapter.

Rigid push–pull rods **31**[34,35] were conceived as shape-persistent α-helix mimics[40] to study the role of dipole–potential interactions for voltage gating in general and the mechanism of action of natural antibiotics[41] in particular. The introduction of a π-donor D at one and a π-acceptor A at the other rod terminus establishes a macrodipole along the rod axis. Different to the macrodipole of α-helices, this rigid-rod dipole is always present without any dependence on conformational changes. Also different to α-helices, the macrodipole can be turned off on demand without major structural changes. Replacement of a sulfide donor D with a sulfone acceptor A, for example, is possible with the formal addition of two atoms and can be done in situ. The *p*-oligophenyl push–pull rods, finally, can serve as an intrinsic fluorescence probe to study dipole–potential interactions on the structural level under conditions that are meaningful with regard to function. In rigid push–pull rods **31**, crown ethers are added along the rigid-rod scaffold to reveal the consequences of dipole–potential interactions on the functional level. Indeed, higher activities were found when a membrane potential was applied, and structural studies confirmed partitioning as the origin of this response.

Originally, rigid-rod β-barrels **32** were introduced to explain puzzling observations with rigid-rod HBCs **29** in planar bilayer conductance experiments.[36] In these barrel–stave supramolecules, rigid rods serve as preorganizing staves that are glued together by antiparallel β-sheet hoops formed by interdigitating peptide strands from neighboring staves. This approach is attractive because the precise positioning of amino-acid residues in β-sheets allows to variably functionalize both inner and outer surface of rigid-rod β-barrels in a rational manner. Because of this key characteristic, the concept of synthetic multifunctional pores could be introduced and developed with rigid-rod β-barrels. Realized examples cover many variations of ion selectivity, voltage gating as well as pore opening and closing in response to chemical stimulation, and catalysis.[12,27] The optical transduction of chemical reactions with synthetic multifunctional pores[40] is particularly attractive because of broad applicability in different fields such as drug discovery (i.e., enzyme inhibitor screening), diagnostics (i.e., multicom-

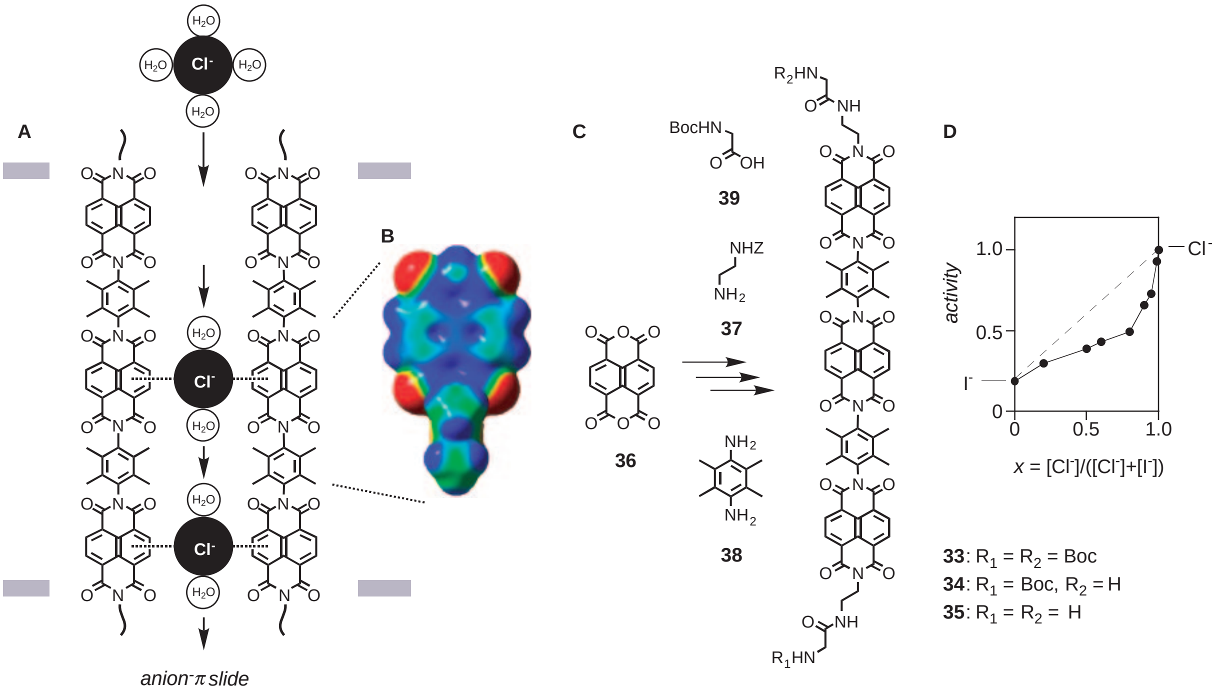

Fig. 3. To introduce the concept of anion–π slides (A) for multiion hopping along transmembrane rigid rods composed of π-acidic NDI modules (B), O-NDI rods **33**–**35** have been synthesized (C). Experimental evidence in support of the concept includes an anomalous mole fraction effect, with reduced activity of mixtures compared to pure ions implying that occupation of multiple aligned sites is required for fast transport of the preferred ion (D). B: DFT computed electrostatic potential maps; red: electron-rich, blue: electron-poor; adapted from Ref. 26, © American Chemical Society 2006.

ponent sensing), and so on.[42–45] A recent example for sensing with refined synthetic multifunctional pores will be discussed later on.[27]

The perfect hoop–stave matching of the hoop–hoop repeat distance of 5.0 Å and the length of the rigid-rod scaffold accounts for the formation of rigid-rod β-barrels **32**. Reduction of the hoop–hoop repeat to ≈3.4 Å by replacement of the β-sheets with π-stacks converts the rigid-rod barrel–stave supramolecule into a rigid-rod π-helix **9**. As elaborated later on, the introduction of transmembrane helical π-stack architecture is of interest to create smart photosystems that can open up into ion channels in response to chemical stimulation.[28]

After this more general overview (Fig. 2), we now zoom in and spotlight three recent studies where naphthalenediimides (NDIs) are introduced as unique, compact, organizable, and colorizable organic n-semiconductors to address specific current challenges in the field. The first topic focuses on synthetic ion channels that introduce anion–π interactions to select for anions and multiion hopping along anion–π slides to preserve speed despite selectivity (Fig. 3).[26] The next topic concerns synthetic pore sensors that introduce aromatic electron donor–acceptor interactions to catch otherwise elusive analytes (Figs. 4–6).[27] The final topic concerns smart photosystems, where photoinduced charge separation is enabled not by covalent donor–acceptor dyads but by the precision of transmembrane rigid-rod π-stack nanoarchitecture (Fig. 7).[28]

Ion Channels and Pores

Pioneered by the groups of Tabushi,[46] Fuhrhop,[47] Kobuke,[48] and others, the creation of new ion channels and pores has become one of the classical applications of synthetic nanoarchitecture in lipid bilayer membranes. Excellent reviews continuously update this field from different points of view.[49–57] Specific topics of current interest that became accessible with the introduction of rigid-rod scaffolds include ion selectivity, voltage gating, membrane recognition, ligand gating, blockage, and catalysis.[12]

Rigid O-NDI rods **6** (Fig. 1) were introduced to create transmembrane anion–π slides.[26] This approach to anion channels was innovative because the elusive anion–π interactions[58,59] are envisioned to select for anions and enable multiion hopping[1,2,60–63] along the π-acidic NDI surfaces along transmembrane O-NDI rods (Fig. 3A).

The concept of rigid O-NDI rods as anion–π slides complements and completes the early breakthroughs with cation–π slides **30** mentioned in the previous section (Fig. 2).[33] However, cation–π interactions are intrinsic characteristics of π-basic aromatics and thus ubiquitous in natural and synthetic multifunctional architecture. In clear contrast, anion–π interactions are theoretically attractive,[54] poorly explored in solution,[55] without reach with biological ion channels and unprecedented in synthetic ion channels.[49–57] Our high-level DFT calculations suggested that the global quadrupole moment of the π-acidic NDIs is as large as $Q_{zz} = +19.4$ B (Buckinghams, Fig. 3B).[26] Clearly beyond the classical hexafluorobenzene ($Q_{zz} = +8.9$ B), this largely positive quadrupole moment promised powerful anion–π interactions. Their magnitude was predicted in the range of cation–π interactions with the complementarily π-basic pyrene ($Q_{zz} = -13.8$ B). The length of the shape-persistent O-NDI rods **33**–**35** was with $l = 32.6$ Å selected to roughly match the thickness of the hydrophobic core of a lipid bilayer membrane.[12,64] These target molecules were readily synthesized from the commercially available dianhydride **36**, amines **37** and **38**, and Boc-glycine **39** (Fig. 3C). Their activity as anion–π slides was determined with large unilamellar vesicles that were loaded with the pH-sensitive fluorescent probe 8-hydroxy-1,3,6-pyrenetrisulfonate (HPTS) and exposed to a pH gradient.[65] Transport activity in this assay is observed as accelerated pH gradient collapse. Overall, O-NDI rods were not very active in this assay. Although difficult to further specify, possible origins of poor activity in this assay include not only poor ion transport ability, but also poor, slow or irreversible partitioning, or "too high" selectivity.[65]

With monomeric rods, activity was highest with one charged but low with two charged termini (**34** > **33** > **35**). These trends can be interpreted as support for the transmembrane orientation of anion–π slides. Namely, they may suggest that one uncharged rod terminus is needed to cross the hydrophobic core of the membrane and adapt the expected transmembrane orientation.[35] One charged terminus may help to loosen up tightly assembled bundles of transmembrane rods and let anions slide through.

The ability of ion channels that discriminate between anions and cations is described as anion/cation selectivity.[65] According to the HPTS assay, not only cationic but also neutral rigid O-NDI rod **33** preferred to transport anions over cations. This anion/cation selectivity was contrary to that of cation–π slide **30** and in support of the occurrence of anion–π interactions.

The ability of anion channels that discriminate between different anions is described in selectivity sequences. Among many theories, variations and refinements available, selectivity sequences are arguably best described as Eisenman topologies.[39,55,63,65,66] Anion selectivity sequences can be classified as halide topologies I–VII.[66] The frequently observed halide sequence I is completely determined by dehydration penalty and often referred to as Hofmeister series. Higher halide sequences dominated by anion binding in the channel are much more difficult to obtain.

The neutral rod **33** discriminated between anions following a halide VI selectivity sequence ($Cl^- > F^- > Br^- > I^-$).[26] Preliminary results indicate that covalent and neutral O-NDI dimers have increased chloride selectivity with unchanged halide VI sequence.[67] Rod **34** with one cationic terminus exhibited a less pronounced halide VI selectivity sequence ($Cl^- > Br^- > F^- > I^-$). These trends suggested that increasing proximity between transmembrane O-NDI slides results in increased selectivity at the cost of reduced apparent activity.

Multiion hopping is the classical biological answer to the dilemma of how to transport fast and selective.[60–63] Strings of ions bound to aligned binding sites have been identified both in cation and anion channels,[1,2] Onsanger's hydrogen-bonded chains may be viewed as variation of the same motive adapted to proton hopping (Fig. 2).[32] In the multiion hopping mechanism, approach of an ion from one side of the membrane causes all ions in the transmembrane string of ions to move one binding site down to cause the release of the last one on the other side of the membrane (Fig. 3A). The classical evidence for a multiion hopping mechanism is AMFE, the anomalous mole fraction effect (Fig. 3D).[60–63] An AMFE stands for reduced activity with mixtures of ions compared to pure ions. This can demonstrate that permanent immobilization of the better binding ion to one single site is insufficient for fast transport. This, in turn, can imply that the occupation of multiple sites along the π-slide is required for fast transport of the preferred ion, this is, the existence of multiion hopping.

Applicability of AMFE to the characterization of synthetic ion channels with the HPTS assay in vesicles was tested with the neutral rod **33** as anion–π slide, Cl^- as the fast and I^- as the slow anion (Fig. 3D). The underadditivity found for mixtures compared to the pure anions revealed a substantial AMFE. This AMFE was naturally the key evidence for the existence of anion–π slides (Fig. 3A). It implied the existence of (at least) three chloride binding sites in close proximity along the ion-conducting pathway. This was compatible with multichloride hopping along the π-acidic NDI modules of anion–π slide **33** and disfavored, for example, the Gly–Boc termini as origin of activity and selectivity.

In research that focuses on the creation of advanced function, experimental evidence in support of that function naturally deserved highest priority.[68] To summarize, this essential line of evidence in support of the concept of rigid O-NDI rods as anion–π slides begins with the confirmation of the possibility of anion–π interactions with the calculation of a strongly positive quadruple moment for the NDI module. The finding that anion selective transport follows a halide VI sequence implied strong anion binding. Increasing selectivity and decreasing activity with removal of one cationic terminus and covalent capture were in support of loosely assembled transmembrane O-NDI rods as active suprastructure. The significant AMFE, finally, demonstrated the occurrence of a multiion hopping mechanism. This finding is equivalent to experimental evidence for the existence of anion–π slides and unprecedented with synthetic ion channels and pores.

Sensors

Synthetic multifunctional pores attract increasing scientific attention because they are of general use in areas such as diagnostics (multicomponent sensing) or drug discovery (inhibitor screening).[43–45] Specific introductory reviews on this topic are available.[69] Without going into extensive details, synthetic pores that open (ligand gating) or close (blockage) became accessible with the discovery of a synthetic route to artificial β-barrels. In these barrel–stave supramolecules, rigid-rod molecules serve as staves (Fig. 4). Interdigitation of short peptides from two neighboring staves **40** produces antiparallel β-sheet hoops. The non-planarity of the *p*-oligophenyl staves, consequence of the biphenyl torsions along the rigid-rod scaffold, prevents the linear self-assembly of the planar β-sheet into precipitating supramolecular polymers and promotes the cylindrical self-assembly into supramolecular oligomers. In the final rigid-rod β-barrel, amino-acid residues decorate both inner and outer barrel surface in well-defined patterns, with both N- and C-terminal residues point outward to avoid internal overcrowding at the rigid-rod turns. Simple modification of amino-acid residues allows to control and vary both physical and chemical properties of outer and inner pore surface in a straightforward and rational manner.

In pore **41**,[70–72] for example, hydrophobic leucine residues

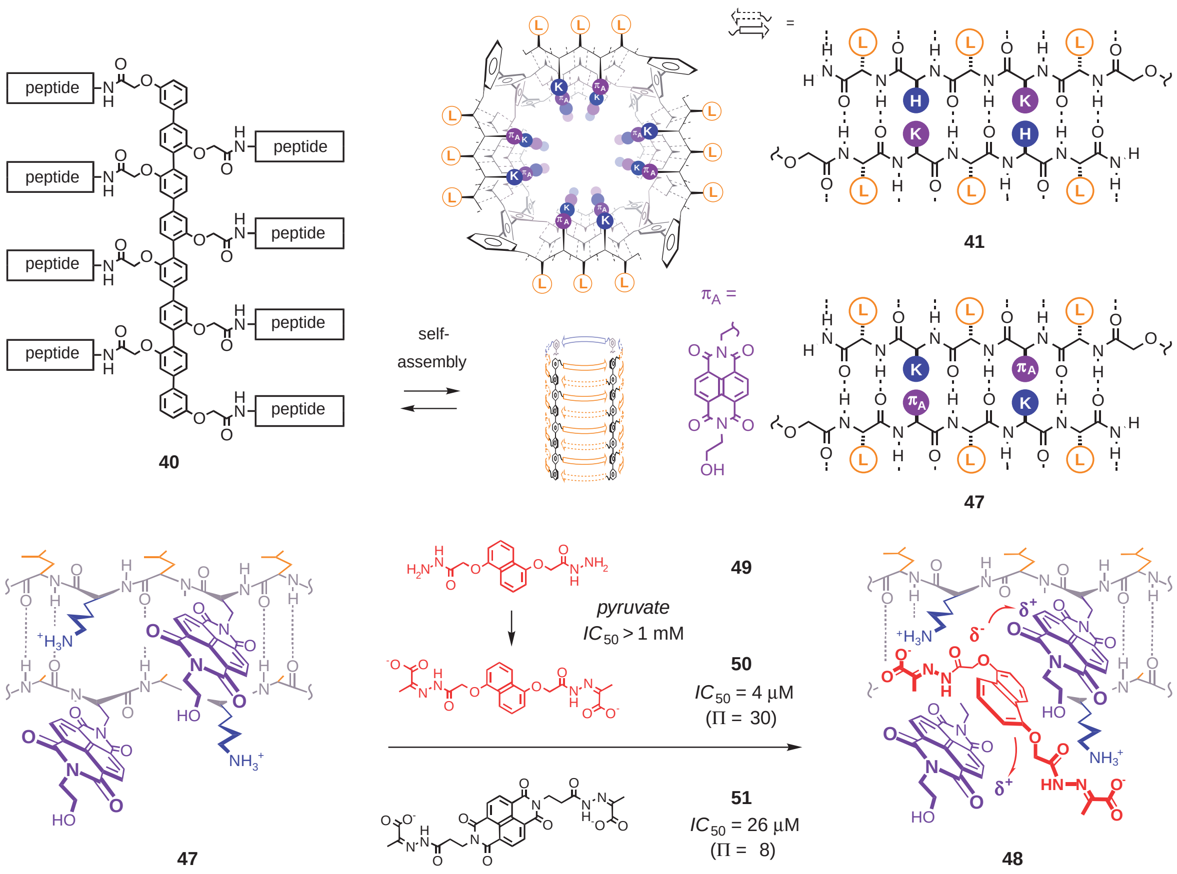

Fig. 4. Synthetic multifunctional pores **41** and **47** are rigid-rod β-barrels, barrel–stave supramolecules that are composed of rigid-rod staves and β-sheet hoops and self-assemble from monomers **40**. Sticky NDI π-clamps are introduced within pore **47** (but not **41**) to catch elusive analytes such as pyruvate by (1) covalent capture with π-basic hydrazide amplifier **49** for molecular recognition as π-basic hydrazone **50** (but not π-acidic hydrazone **51**) by aromatic electron donor–acceptor interactions in complex **48**. See Fig. 6 for molecular dynamics simulations of inclusion complex **48**.

are placed at the outer barrel surface to maximize interactions with the surrounding bilayer without significant barrel destabilization. Histidine–lysine dyads were introduced at the inner barrel surface to recognize and transform molecules that are passing by, through the pore and across the bilayer membrane. Pore **41** was found to recognize ATP as efficiently as expected.[71] Blockage of the same pore by ADP was clearly less effective. This substantial discrimination made the conversion of ATP into ADP detectable as "fluorogenic" opening of pore **41**, that of ADP into ATP as closing of the same pore (Fig. 5). In this process, pore **41** acts as optical transducer of a chemical reaction. ATP/ADP discrimination is of interest, for example, to detect the activity of enzymes such as kinases that catalyze this reaction. Such optical transduction of enzyme activity with pores is of use to screen for inhibitors of enzymes that are attractive targets for drug discovery but otherwise difficult to address.[43–45,73–76]

The combination of optical transduction by synthetic pores with signal generation by enzymes is of interest for sensing applications.[43–45] Sugar sensing by pore **41** in soft drinks was selected as illustrative example (Fig. 5).[71] Coca-Cola, was incubated first with invertase to convert sucrose **42** into glucose **43** and fructose **44**. Phosphorylation of the obtained monosaccharides with hexokinase gave glucose-6-phosphate **45** and fructose-6-phosphate **46**. Conversion of the good pore blocker ATP into the poor blocker ADP during saccharide phosphorylation was observable with the "naked eye" as fluorogenic pore opening (Fig. 5B).

Although our research devoted to the creation of advanced function,[68] insights on the structural level do exist. The clear highlight among a rich and consistent collection of direct evidence are AFM snapshots obtained by Yashima, Kumaki, and co-workers that show a single polymer blocker entering and moving through a single pore **41**.[72]

The use of synthetic pores as optical transducers of chemical reactions is scientifically attractive because the general applicability of this approach is comparable with chromatographic methods such as TLC or HPLC. Compatibility with enzymes has been demonstrated exhaustively, and the implementation of numerous and diverse practical screening and sensing applications is ongoing. For molecular recognition by various rigid-rod β-barrel pores, multiple ion pairing has been emphasized. Dramatically changed characteristics upon replacement of the internal lysines of **41** with arginines, for instance, prompted us to explore the role of counter ions for oligoarginine function in a very general context, reaching cell-penetrating peptides (in collaboration with the Futaki group)[77,78] to sensing applications (in collaboration with the Miyatake

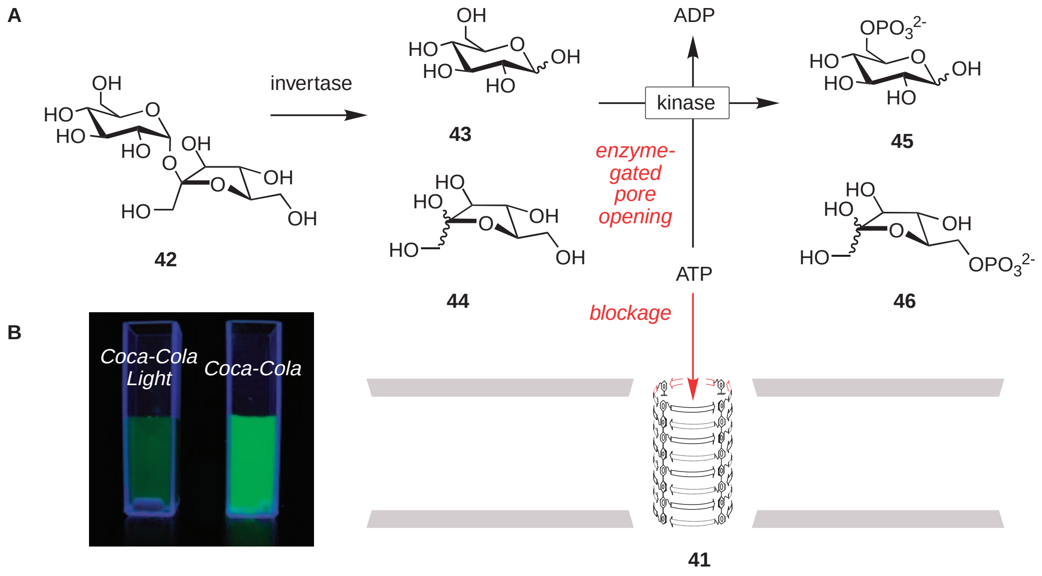

Fig. 5. Synthetic multifunctional pore **41** as sugar sensor. Treatment with first invertase and then hexokinase reveals the presence of sucrose **42** in Coca-Cola (B) because of fluorogenic efflux of entrapped fluorescein though the pore sensor in response to the conversion of the good blocker ATP into the poor blocker ADP during the second process (A). Coca-Cola Light treated the same way does not fluoresce because the good blocker ATP is not consumed in the absence of sucrose and the pore thus remains closed. Adapted from Ref. 67, © American Chemical Society 2005.

group).[73] For molecular recognition by the complementary aromatic electron donor–acceptor interactions, we recently synthesized pore **47** with NDIs at the inner pore surface.[27]

In pore **47**, the NDIs were diagonally positioned on one face of a β-sheet (Figs. 4 and 6). Like this, they are too far apart to π-stack and thus ideally placed to serve as π-clamps. π-Clamps, also referred to as tweezers, clips, clefts, or jaws,[79–87] are quite popular bifunctional acyclic hosts that form face-to-face complexes with intercalating aromatic guest (e.g., **48**, Fig. 4). Different to molecular recognition by caffeine,[79] acridine,[80] phenantrene,[80] glycoluryl,[81] naphthalene,[82] anthracene,[82] pyrene,[83] porphyrin,[84–86] or pentafluorophenyl[87] tweezers, different also to Butterfield and Waters' pioneering tryptophan clamps on a β-sheet scaffold,[88] π-clamping with the "adhesive," π-acidic NDI dimers as such has never been studied systematically. However, the classical charge-transfer (CT) complexes with π-basic dialkoxynaphthalenes (DANs) have been used extensively and successfully in supramolecular architecture. Pioneered by Iverson's elegant foldamers,[89] examples include the creation of double helices,[89] barrel–stave supramolecules,[31] rotaxanes or catenanes[90] that can act as shuttles,[90] stimuli-responsive gels,[91] or ligand-gated ion channels.[31]

Molecular dynamics simulations were compatible with the possibility of adhesive π-clamping of up to two within pore **47**. In Fig. 6, the DAN moiety of the substrate and clamping NDIs are highlighted to illustrate the key π–π interactions in this supramolecular complex. To explore existence, significance and usefulness of adhesive π-clamping within pore **47** experimentally, we developed an in situ approach for rapid screening of blocker libraries. As expected from extensive precedence,[92–97] reversible reaction of the newly synthesized π-basic DAN dihydrazide **49** with ketones such as pyruvate provided rapid access to a focused library of DAN and NDI blockers of different bulk and charge such as hydrazone **50**.[27]

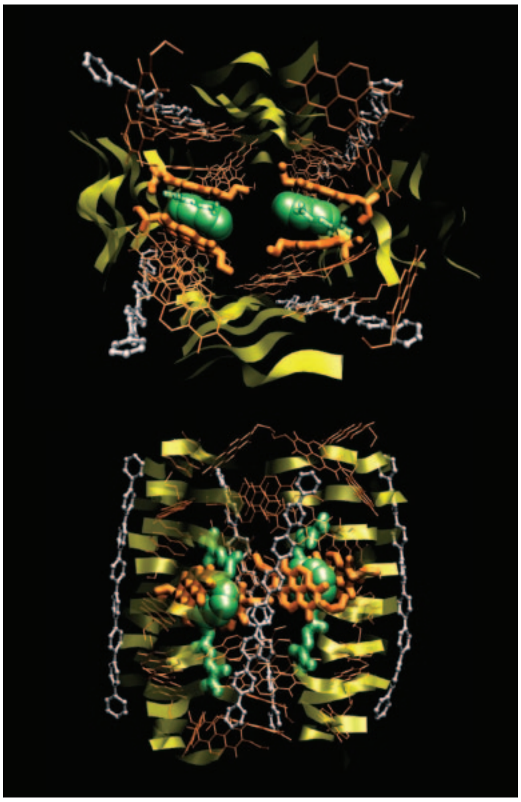

Fig. 6. Molecular dynamics simulations of synthetic multifunctional pore **47** in side (bottom) and axial view (top) with rigid-rod staves in silver (ball-and-stick), β-sheet hoops in gold (ribbons) and NDI clamps in orange (wires) with two bound hydrazones **50** in lime (space filling). See Fig. 4 for chemical structures.

The π-basic hydrazone **50** blocked pore **47** with π-acidic NDI clamps with an inhibitory concentration $IC_{50} = 4\,\mu M$. This finding was interesting but naturally insufficient as evidence for operational adhesive π-clamping. The observation that blockage of the clamp-free pore **41** by the same blocker was 30-times weaker was more convincing and used to define a clamping factor $\prod$. To explore the adhesiveness of π-clamping within pore **47**, comparison with simple IC_{50}'s of π-acidic blockers such as the 7.5-times larger one of hydrazone **51** was insufficient. To exclude contributions from effects other than aromatic electron donor–acceptor interactions, comparison of clamping factors $\prod$ of π-basic blockers such as **50** and π-acidic blockers such as **51** was necessary. The found increasing clamping factors with increasing π-basicity of the blocker confirmed contributions from aromatic electron donor–acceptor interactions to π-clamping within the π-acidic synthetic pore **47**. Control experiments showed that aliphatic rather than aromatic blockers were ineffective and that proximal ion pairing strengthens rather than weakens adhesive π-clamping. As far as sensing applications are concerned, we point out that the covalent capture of pyruvate as hydrazone **50** increases the sensitivity by more than three orders of magnitude (i.e., >1000-times!). The product of several enzymatic transformation, pyruvate is an interesting analyte in biosensing. Efforts to use hydrazide amplifiers and π-clamping within synthetic pores in sensing applications are ongoing, preliminary results are highly encouraging.[45]

Photosystems

According to pertinent reports,[98] a major effort in basic research on smart optoelectric nanomaterials is needed today to meet tomorrows energy demand in a sustainable way. The notion that the precision of nanoarchitecture directly determines advanced function has never been more true than with molecular (opto)electronics such as solar cells. Unidirectional charge mobility in π-stacks can be as good as in conjugated polymers, with precise self-organization, sample conditions and sample history being as critical as monomer structure.[99,100] Charge mobilities in advanced discotic liquid crystalline π-stacks, for example, are with up to $1\,cm^2\,V^{-1}\,s^{-1}$ clearly beyond the reported $\approx 0.1\,cm^2\,V^{-1}\,s^{-1}$ for solution-synthesized conjugated polymers such as liquid-crystalline polyfluorene and poly(phenylenevinylene). Compared to conjugated polymers, self-organization in refined coronene, porphyrin, or phthalocyanine π-stack architecture can overcompensate the weaker electronic coupling between monomer units.

Classical approaches to synthetic photosystems focus, however, on covalent chemistry to place an acceptor on one side and, in some cases, an electron donor on the other side of one or several chromophores.[101–105] Upon excitation with light, intramolecular transfer of an electron to the acceptor and, eventually, coinciding electron transfer from the donor to the photooxidized chromophore causes a transient separation of charges. Donor and acceptor are selected to convert as much photonic energy as possible into chemical energy. Strategies to prevent instantaneous charge recombination include increasing donor–acceptor distance and decreasing reorganization energies to enter the Marcus inverted region. In synthetic photosystems, porphyrins are most frequent chromophores, fullerenes have replaced quinones as most common acceptors. Studied with regard to photovoltaics in several groups including Fukuzumi[102] and Kobuke,[103] photosynthesis in lipid bilayer membranes with covalent donor–chromophore–acceptor triads has been pioneered by Gust, Moore, and Moore.[101]

Support for the functional significance of advanced nanoarchitecture for molecular (opto)electronics came from studies on core-substituted perylenediimides (PDIs) in the Wasielewski group.[106] Covalently enforced co-facial π-stacking was shown to produce characteristics such as excited-state symmetry breaking, ultrafast charge separation ($\tau = 0.52\,ps$) and delayed recombination ($\tau = 222\,ps$). Charge separation within donor–acceptor-free chromophore stacks rather than the classical donor–chromophore–acceptor triads is naturally short but attractive because no energy is lost.

One important difference of NDIs compared to core-substituted PDIs is their planarity.[30,105,107] This planarity was expected to maximize co-facial π-stacking and, therefore, charge separation in photoactive nanoarchitecture. Indications for conductive NDI stacks were secured early on with the appearance of a strong Near-IR-band at 1140 nm in response to electrochemical or chemical one-electron reduction.[108] The discovery of π-stacks of NDI radical anions was significant because, different to p-conducting polymers or π-stacks, n-conducting π-stacks or polymers are usually not air stable. Maximal electron mobilities of NDI films were with $0.12\,cm^2\,V^{-1}\,s^{-1}$, clearly beyond the $\leq 0.02\,cm^2\,V^{-1}\,s^{-1}$ of π-conjugated n-semiconductors.[109]

The recently discovered synthetic access to blue, red, and yellow fluorophores with accessible oxidation as well as reduction potentials spotlighted NDI as exceptionally compact, i.e., atom-efficient potential chlorophyll mimic.[30] Moreover, the planarity of core-substituted NDIs promised access to nanoarchitecture that determines conductivity as well as photoactivity but is difficult with the non-planar PDIs. These high expectations lead us to the third and arguably most adventurous application of NDIs in multifunctional rigid-rod nanoarchitectonics, i.e., the creation of smart photosystem **9** that can open up into ion channels in response to chemical stimulation (Fig. 7).[28]

The idea to replace β-sheets in rigid-rod β-barrels with π-stacks was the key to photoactive rigid-rod π-stack nanoarchitecture. In rigid-rod β-barrels, β-sheets serve as hoops that hold the rigid-rod staves together. The distance between two strands in a β-sheet is $\approx 5\,Å$ (Fig. 2). For an 8-stranded β-sheet, this gives a length of $\approx 35\,Å$. This length matches precisely the length of the *p*-octiphenyl stave (34 Å). This hoop–stave matching is the reason why rigid-rod β-barrels are barrels and not helices. Replacement of β-sheets with π-stacks significantly disturbs this hoop–stave matching. The distance between two face-to-face stacked aromatics is $\approx 3.4\,Å$ (Fig. 2). For an 8-membered π-stack, this gives a length of $\approx 24\,Å$. This is clearly shorter than a *p*-octiphenyl rod. To maximize face-to-face π-stacking, the resulting hoop–stave mismatch was expected to twist rigid-rod π-barrels into rigid-rod π-helices **4**.

The question whether or not this formal barrel → helix transition would increase or decrease the central pore of rigid-rod β-barrels was intriguing. In biology, large mechanosen-

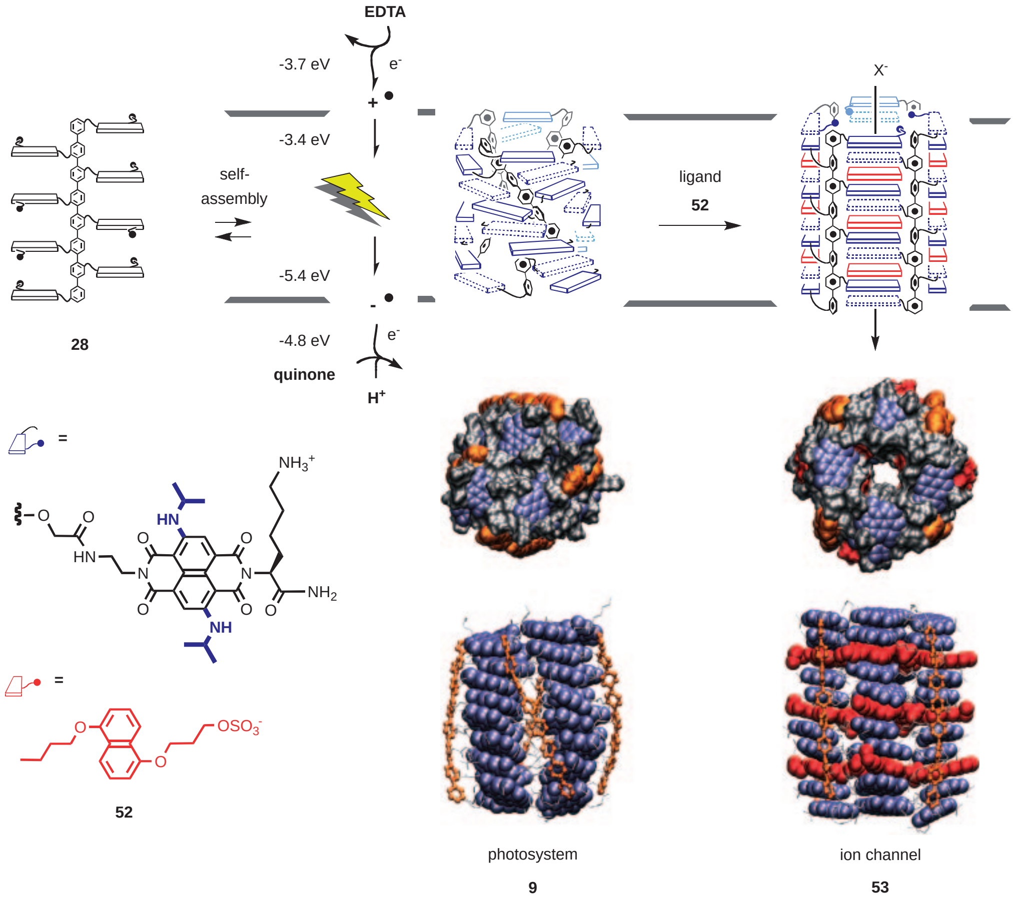

Fig. 7. Self-assembly of rigid rod **28** into quadruple π-*M*-helix **9**, and helix → barrel transition into open ion channel **53** in response to the intercalation of ligands **52** (compare Scheme 1). In the shown application of photosystem **9**, transmembrane photoinduced electron transfer from EDTA donors to quinone acceptors Q is measured with the pH sensitive probe HPTS as formal proton pumping with light across lipid bilayers. Molecular models of photosystem **9** and ion channel **53** show solvent-accessible surfaces (grey, axial views, top) and tube projections (white, side views, bottom) with highlighted NDIs (blue), DANs (red, both space filling) and *p*-octiphenyls (gold); adapted from Ref 28, © American Association for the Advancement of Science.

sitive ion channels (MscL) provide the outstanding example for pore opening in response to barrel → helix transition.[4] However, support for pore closing in response to barrel → helix transition could be found as well, for example in the admittedly more complex acetylcholine receptor.[5] For the occurrence of pore opening or closing upon barrel → helix transition, what seems to matter most is the stickiness of the involved staves. With slippery rods as in the MscL, allowed rod-on-rod sliding motions during barrel → helix transition result in pore opening. With sticky rods, these sliding motions are forbidden, and pore closing is the only alternative left. This pore closing by barrel → helix transition with sticky rods is perfectly simulated in a hyperboloid (with inelastic staves and movable end-caps). In rigid-rod π-stack nanoarchitecture **9**, the rods are about as sticky as it gets. Barrel → helix transition with π-stack hoops should thus be "hyperboloidal," the pore within rigid-rod π-helix **9** be closed.

The transmembrane but impermeable π-stack nanoarchitecture **9** obtained from hyperboloidal barrel → helix transition appeared ideal for artificial photosynthesis (Fig. 7).[28] Moreover, elimination of hoop–stave mismatch by intercalation of ligands **52** should trigger helix → barrel transition to open photosystem **9** up into barrel–stave ion channel **53** (Fig. 7).[31] Central in chemistry and biology of oligonucleotides, we highlight that such stimuli-responsive π-stack nanoarchitecture is rare in biomembrane function, not to speak of synthetic multifunctional architecture in biomembrane models.

The planar, electron-deficient NDIs appeared ideal for favorable self-assembly of monomeric *p*-octiphenyl rods **28** into π-helix **9**; amides were added at both sides to orient the NDI stacks with flancking H-bonded chains.[28] Similar to chlorophyll and core-substituted *N*,*N*-PDIs but more compact (i.e., "atom-efficient"), the deep blue color and blood red emission obtained with dialkylamine core substitution appeared ideal to capture photonic energy. Moreover, introduction of the π-donors in the core of *N*,*N*-NDIs move both reduction and oxidation potential into regions that are perfect for artificial photosynthesis. In nanoarchitecture **9**, the stacked chromophore array is thus expected to serve not only as chromophore but also as electron acceptor and electron donor, with excited electrons simply hopping away along the conducting, π-acidic stack, electrostatically stabilized by the hole left behind. This transient photoinduced charge separation in advanced nanoarchitecture **9** without extra donors and acceptors was thus expected to occur with minimal loss of photonic energy (i.e., "energy-maximized"). Time-resolved fluorescence and transient absorption measurements confirmed that this is the case: Upon irradiation of **9**, ultrafast (<2 ps) charge separation occurs quantitatively (>97%) and lasts relatively long (61 ps).

To elaborate on artificial photosynthesis with rigid-rod π-helix **9**, vesicles were surrounded with electron donors (EDTA, ethylenediaminetetraacetate; $E_{1/2}$ (NHE) $\approx +1.0$ V) and loaded with electron acceptors (1,4-naphthoquinone-2-sulfonate; $E_{1/2} \approx -0.06$ V). Their redox potentials were selected to oxidize the charge-separated, transmembrane photosystem **9** on the one side and fill the hole on the other. Thermally unfavorable, this transmembrane photoredox process converts photonic into chemical energy. To detect photosynthetic activity, the vesicles were further loaded with a fluorescent pH meter, i.e., HPTS. Increasing pH in response to irradiation with red light demonstrated proton consumption during intravesicular quinone reduction, that is, photosynthetic activity of rigid-rod π-stack architecture **9**.

The transmembrane pH gradient created with light and photosystem **9** was readily removed by transforming the latter into an ion channel. Electron-rich DANs **52** were used as ligands to intercalate into π-helix **9**. As elaborated above, such elimination of the hoop–stave mismatch was expected to cause the opening into the barrel–stave ion channel **53**. The helix → barrel transition from photosystem **9** to ion channel **53** turned out to be highly cooperative, highly sensitive, and highly selective with regard to both ligand and channel structure. The obtained ion channels were small, anion selective, and surprisingly homogenous.[28,31,110–112]

Conclusion

Rigid-rod molecules as priviledged scaffolds in lipid bilayer membrane as compartmentalizing platform emerge as attractive strategy to create advanced nanoarchitecture with interesting functions. Realized examples include a rich collection of barrels, helices, stacks, slides, and wires that can act as ion channels, sensors, photosystems, and catalysts with a broad variety of distinct characteristics.

In this review, special emphasis is on recent studies with naphthalenediimides (NDIs). As transmembrane rigid rods, the π-acidic NDIs are attractive because they introduce the otherwise inaccessible anion–π interactions to select for anions.[26] As π-clamps within rigid-rod pore sensors, NDIs are attractive because they can catch and amplify otherwise elusive analytes by means of aromatic electron donor–acceptor interactions.[27] As π-stacks between transmembrane rigid rods, NDIs are attractive because they can act as smart photosystems that can open up into ion channels in response to chemical stimulation.[28]

These specific examples with multifunctional NDI nanoarchitecture are not only interesting to outline the potential of this research to contribute to advanced functional materials such as multianalyte sensors or solar cells. They also make us wonder about an overwhelming chemical space waiting to be exploited. For example, from the structural point of view, O-NDIs are just one out of many possible rigid-rod molecules beyond p-oligophenyls that promise access to new structures with new functions.[15–25] The imaginable variability of hoops beyond β-sheets in barrel–stave supramolecules simply enormous. Access to transmembrane rigid-rod π-stack architecture is naturally not limited to NDI π-stacks.[113] Even in the limited suprastructural space of p-oligophenyl β-barrels, internal NDI π-clamps are just one out of many possibilities to create refined active sites.[114,115]

As far as functional sophistication and diversity are concerned, the discussed examples for ion channels, sensors, and photosystems hint at enormous potential available in both directions. With regard to sophistication, the advanced situation with channels and pores invites to tackle specific challenges such as control over partitioning[70] or the detection of catalysis within pores on the single molecule level.[116,117] The exceptional potential of the general optical transduction of reactions with rigid-rod pores for applications in domains such as drug discovery (enzyme inhibitor screening), diagnostics (multianalyte sensing), and so on invites to elaborate on diversity.[44,45] This may include variation in mode of detection (conductance),[117–119] membranes (solid-supported,[118,119] planar,[117] polymersomes),[120–122] pores,[73] reactions[43–45,73–76] (enantioselectivity),[45] enzymes for inhibitor screening,[73–76] enzymes for signal generation,[43–45,73–76] reactive amplifiers, analytes, matrix, and so on.[44,45] The mainly academic nature of artificial photosynthesis in lipid bilayers, finally, invites to apply the lessons learned to advanced rigid-rod nanoarchitecture on conducting surfaces such as gold or ITO[102,103] with the hope to end up with photovoltaic devices.

We warmly thank all past co-workers and all past and present collaborators for invaluable contributions, and Swiss NSF for financial support.

References

† Dedicated to Professor Yoshiaki Kobuke on the occasion of his 65th birthday.

1 R. Dutzler, *FEBS Lett.* **2004**, *564*, 229.

2 Y. Jiang, V. Ruta, J. Chen, A. Lee, R. MacKinnon, *Nature* **2003**, *423*, 42.

3 S. Khademi, J. O'Connell, III, J. Remis, Y. Robles-Colmenares, L. J. W. Miercke, R. M. Stroud, *Science* **2004**, *305*, 1587.

4 E. Perozo, D. M. Cortes, P. Sompornpisut, A. Kloda, B. Martinac, *Nature* **2002**, *418*, 942.

5 A. Miyazawa, Y. Fujiyoshi, N. Unwin, *Nature* **2003**, *423*, 949.

6 V. Koronakis, A. Sharff, E. Koronakis, B. Luisi, C. Hughes, *Nature* **2000**, *405*, 914.

7 C. J. Oomen, P. van Ulsen, P. van Gelder, M. Feijen, J. Tommassen, P. Gros, *EMBO J.* **2004**, *23*, 1257.

8 J. Deisenhofer, H. Michel, *Science* **1989**, *245*, 1463.

9 N. Nelson, A. Ben-Shem, *Nat. Rev. Mol. Cell Biol.* **2004**, *5*, 971.

10 P. Jordan, P. Fromme, H.-T. Witt, O. Klukas, W. Saenger, N. Krauss, *Nature* **2001**, *411*, 909.

11 N. Sakai, K. C. Brennan, L. A. Weiss, S. Matile, *J. Am. Chem. Soc.* **1997**, *119*, 8726.

12 N. Sakai, J. Mareda, S. Matile, *Acc. Chem. Res.* **2005**, *38*, 79.

13 D. J. Hill, M. J. Mio, R. B. Prince, T. S. Hughes, J. S. Moore, *Chem. Rev.* **2001**, *101*, 3893.

14 S. H. Gellman, *Acc. Chem. Res.* **1998**, *31*, 173.

15 P. F. H. Schwab, M. D. Levin, J. Michl, *Chem. Rev.* **1999**, *99*, 1863.

16 *Electronic Materials: The Oligomer Approach*, ed. by K. Müllen, G. Wegner, Wiley-VCH, Weinheim, **1998**.

17 M. B. Nielsen, F. Diederich, *Chem. Rec.* **2002**, *2*, 189.

18 F. Cacialli, J. S. Wilson, J. J. Michels, C. Daniel, C. Silva, R. H. Friend, N. Severin, P. Samori, J. P. Rabe, M. J. O'Connell, P. N. Taylor, H. L. Anderson, *Nat. Mater.* **2002**, *1*, 160.

19 W.-Y. Yang, J.-H. Ahn, Y.-S. Yoo, N.-K. Oh, M. Lee, *Nat. Mater.* **2005**, *4*, 399.

20 K. Tsubaki, K. Takaishi, H. Tanaka, M. Miura, T. Kawabata, *Org. Lett.* **2006**, *8*, 2587.

21 N. G. Pschirer, C. Kohl, F. Nolde, J. Qu, K. Müllen, *Angew. Chem., Int. Ed.* **2006**, *45*, 1401.

22 P. E. Eaton, K. Pramod, T. Emrick, R. Gilardi, *J. Am. Chem. Soc.* **1999**, *121*, 4111.

23 L. L. Miller, B. Zinger, J. S. Schlechte, *Chem. Mater.* **1999**, *11*, 2313.

24 M. J. Ahrens, L. E. Sinks, B. Rybtchinski, W. Liu, B. A. Jones, J. M. Giaimo, A. V. Gusev, A. J. Goshe, D. M. Tiede, M. R. Wasielewski, *J. Am. Chem. Soc.* **2004**, *126*, 8284.

25 N. Aratani, A. Osuka, Y. H. Kim, D. H. Jeong, D. Kim, *Angew. Chem., Int. Ed.* **2000**, *39*, 1458.

26 V. Gorteau, G. Bollot, J. Mareda, A. Perez-Velasco, S. Matile, *J. Am. Chem. Soc.* **2006**, *128*, 14788.

27 H. Tanaka, S. Litvinchuk, D.-H. Tran, G. Bollot, J. Mareda, N. Sakai, S. Matile, *J. Am. Chem. Soc.* **2006**, *128*, 16000.

28 S. Bhosale, A. L. Sisson, P. Talukdar, A. Fürstenberg, N. Banerji, E. Vauthey, G. Bollot, J. Mareda, C. Röger, F. Würthner, N. Sakai, S. Matile, *Science* **2006**, *313*, 84.

29 B. Baumeister, N. Sakai, S. Matile, *Org. Lett.* **2001**, *3*, 4229.

30 F. Würthner, S. Ahmed, C. Thalacker, T. Debaerdemaeker, *Chem. Eur. J.* **2002**, *8*, 4742.

31 P. Talukdar, G. Bollot, J. Mareda, N. Sakai, S. Matile, *J. Am. Chem. Soc.* **2005**, *127*, 6528.

32 L. A. Weiss, N. Sakai, B. Ghebremariam, C. Ni, S. Matile, *J. Am. Chem. Soc.* **1997**, *119*, 12142.

33 M. M. Tedesco, B. Ghebremariam, N. Sakai, S. Matile, *Angew. Chem., Int. Ed.* **1999**, *38*, 540.

34 J.-Y. Winum, S. Matile, *J. Am. Chem. Soc.* **1999**, *121*, 7961.

35 N. Sakai, D. Gerard, S. Matile, *J. Am. Chem. Soc.* **2001**, *123*, 2517.

36 N. Sakai, N. Majumdar, S. Matile, *J. Am. Chem. Soc.* **1999**, *121*, 4294.

37 Y. Tanaka, Y. Kobuke, M. Sokabe, *Angew. Chem., Int. Ed. Engl.* **1995**, *34*, 693.

38 R. A. Kumpf, D. A. Dougherty, *Science* **1993**, *261*, 1708.

39 G. Eisenman, R. Horn, *J. Membr. Biol.* **1983**, *76*, 197.

40 J. M. Davis, L. K. Tsou, A. D. Hamilton, *Chem. Soc. Rev.*, in press.

41 P. Juvvadi, S. Vunnam, R. B. Merrifield, *J. Am. Chem. Soc.* **1996**, *118*, 8989.

42 G. Das, P. Talukdar, S. Matile, *Science* **2002**, *298*, 1600.

43 G. Das, S. Matile, *Chem. Eur. J.* **2006**, *12*, 2936.

44 S. Matile, H. Tanaka, S. Litvinchuk, *Analyte Sensing across Membranes with Artificial Pores* in *Chemical Sensor Systems*, ed. by T. Schrader, *Top. Curr. Chem.*, in press.

45 S. Litvinchuk, H. Tanaka, T. Miyatake, D. Pasini, T. Tanaka, G. Bollot, J. Mareda, S. Matile, in preparation.

46 I. Tabushi, Y. Kuroda, K. Yokota, *Tetrahedron Lett.* **1982**, *23*, 4601.

47 J.-H. Fuhrhop, U. Liman, V. Koesling, *J. Am. Chem. Soc.* **1988**, *110*, 6840.

48 Y. Kobuke, K. Ueda, M. Sokabe, *J. Am. Chem. Soc.* **1992**, *114*, 7618.

49 P. Scrimin, P. Tecilla, *Curr. Opin. Chem. Biol.* **1999**, *3*, 730.

50 G. W. Gokel, A. Mukhopadhyay, *Chem. Soc. Rev.* **2001**, *30*, 274.

51 U. Koert, L. Al-Momani, J. R. Pfeifer, *Synthesis* **2004**, 1129.

52 S. Matile, A. Som, N. Sordé, *Tetrahedron* **2004**, *60*, 6405.

53 A. L. Sisson, M. R. Shah, S. Bhosale, S. Matile, *Chem. Soc. Rev.* **2006**, *35*, 1269.

54 T. M. Fyles, *Chem. Soc. Rev.* **2007**, *36*, 335.

55 A. P. Davis, D. N. Sheppard, B. D. Smith, *Chem. Soc. Rev.* **2007**, *36*, 348.

56 J. T. Davis, G. P. Spada, *Chem. Soc. Rev.* **2007**, *36*, 296.

57 K. Kim, N. Selvapalam, Y. H. Ko, K. M. Park, D. Kim, J. Kim, *Chem. Soc. Rev.* **2007**, *36*, 267.

58 C. Garau, D. Quiñonero, A. Frontera, P. Ballester, A. Costa, P. M. Deyà, *J. Phys. Chem. A* **2005**, *109*, 9341.

59 R. M. Fairchild, K. T. Holman, *J. Am. Chem. Soc.* **2005**, *127*, 16364.

60 B. Hille, W. Schwarz, *J. Gen. Physiol.* **1978**, *72*, 409.

61 J. A. Tabcharani, J. M. Rommens, Y.-X. Hou, X.-B. Chang, L.-C. Tsui, J. R. Riordan, J. W. Hanrahan, *Nature* **1993**, *366*, 79.

62 C. Miller, *J. Gen. Physiol.* **1999**, *113*, 783.

63 Z. Qu, H. C. Hartzell, *J. Gen. Physiol.* **2000**, *116*, 825.

64 B. Ghebremariam, V. Sidorov, S. Matile, *Tetrahedron Lett.* **1999**, *40*, 1445.

65 S. Matile, N. Sakai, *The Characterization of Synthetic Ion Channels and Pores* in *Analytical Methods in Supramolecular Chemistry*, ed. by C. A. Schalley, Wiley, Weinheim, **2007**, pp. 391–418.

66 E. M. Wright, J. M. Diamond, *Physiol. Rev.* **1977**, *57*, 109.

67 V. Gorteau, S. Matile, in preparation.

68 Y. Baudry, G. Bollot, V. Gorteau, S. Litvinchuk, J. Mareda, M. Nishihara, D. Pasini, F. Perret, D. Ronan, N. Sakai, M. R. Shah, A. Som, N. Sordé, P. Talukdar, D.-H. Tran, S. Matile, *Adv. Funct. Mater.* **2006**, *16*, 169.

69 N. Sakai, S. Matile, *Chem. Commun.* **2003**, 2514.

70 S. Litvinchuk, G. Bollot, J. Mareda, A. Som, D. Ronan, M. R. Shah, P. Perrottet, N. Sakai, S. Matile, *J. Am. Chem. Soc.* **2004**, *126*, 10067.

71 S. Litvinchuk, N. Sordé, S. Matile, *J. Am. Chem. Soc.* **2005**, *127*, 9316.

72 J. Kumaki, E. Yashima, G. Bollot, J. Mareda, S. Litvinchuk, S. Matile, *Angew. Chem., Int. Ed.* **2005**, *44*, 6154.

73 T. Miyatake, M. Nishihara, S. Matile, *J. Am. Chem. Soc.* **2006**, *128*, 12420.

74 J. P. Goddard, J.-L. Reymond, *Curr. Opin. Biotechnol.* **2004**, *15*, 314.

75 A. Ojida, I. Hamachi, *Bull. Chem. Soc. Jpn.* **2006**, *79*, 35.

76 S. Tamaru, S. Kiyonaka, I. Hamachi, *Chem. Eur. J.* **2005**, *11*, 7294.

77 T. Takeuchi, M. Kosuge, A. Tadokoro, Y. Sugiura, M. Nishi, M. Kawata, N. Sakai, S. Matile, S. Futaki, *ACS Chem. Biol.* **2006**, *1*, 299.

78 N. Sakai, S. Futaki, S. Matile, *Soft Matter* **2006**, *2*, 636.

79 C.-W. Chen, H. W. Whitlock, *J. Am. Chem. Soc.* **1978**, *100*, 4921.

80 S. C. Zimmerman, K. W. Saionz, *J. Am. Chem. Soc.* **1995**, *117*, 1175.

81 A. E. Rowan, J. A. A. W. Elemans, R. J. M. Nolte, *Acc. Chem. Res.* **1999**, *32*, 995.

82 F.-G. Klärner, B. Kahlert, *Acc. Chem. Res.* **2003**, *36*, 919.

83 H. M. Colquhoun, Z. Zhu, D. J. Williams, *Org. Lett.* **2003**, *5*, 4353.

84 H.-J. Schneider, L. Tianjun, M. Sirish, V. Malinovski, *Tetrahedron* **2002**, *58*, 779.

85 D. Sun, F. S. Tham, C. A. Reed, L. Chaker, P. D. W. Boyd, *J. Am. Chem. Soc.* **2002**, *124*, 6604.

86 S. Yagi, M. Ezoe, I. Yonekura, T. Takagishi, H. Nakazumi, *J. Am. Chem. Soc.* **2003**, *125*, 4068.

87 T. Korenaga, Y. Kawauchi, T. Kosaki, T. Ema, T. Sakai, *Bull. Chem. Soc. Jpn.* **2005**, *78*, 2175.

88 S. M. Butterfield, M. L. Waters, *J. Am. Chem. Soc.* **2003**, *125*, 9580.

89 G. J. Gabriel, B. L. Iverson, *J. Am. Chem. Soc.* **2002**, *124*, 15174.

90 S. A. Vignon, T. Jarrosson, T. Iijima, H. R. Tseng, J. K. M. Sanders, J. F. Stoddart, *J. Am. Chem. Soc.* **2004**, *126*, 9884.

91 P. Mukhopadhyay, Y. Iwashita, M. Shirakawa, S. Kawano, N. Fujita, S. Shinkai, *Angew. Chem., Int. Ed.* **2006**, *45*, 1592.

92 J. Shao, J. P. Tam, *J. Am. Chem. Soc.* **1995**, *117*, 3893.

93 E. C. Rodriguez, K. A. Winans, D. S. King, C. R. Bertozzi, *J. Am. Chem. Soc.* **1997**, *119*, 9905.

94 V. W. Cornish, K. M. Hahn, P. G. Schultz, *J. Am. Chem. Soc.* **1996**, *118*, 8150.

95 P. T. Corbett, J. Leclaire, J. Vial, K. R. West, J.-L. Wietor, J. K. M. Sanders, S. Otto, *Chem. Rev.* **2006**, *106*, 3652.

96 B. Levrand, Y. Ruff, J.-M. Lehn, A. Herrmann, *Chem. Commun.* **2006**, 2965.

97 A. Som, S. Matile, *Eur. J. Org. Chem.* **2002**, 3874.

98 Basic Research Needs for Solar Energy Utilization, US Department of Energy, **2005**, http://www.sc.doe.gov/bes/reports/files/SEU_rpt.pdf; G. Hess, *Chem. Eng. News* **2005**, *83*, 12.

99 J. M. Warman, M. P. de Haas, G. Dicker, F. C. Grozema, J. Piris, M. G. Debije, *Chem. Mater.* **2004**, *16*, 4600.

100 F. J. M. Hoeben, P. Jonkheijm, E. W. Meijer, A. P. H. J. Schenning, *Chem. Rev.* **2005**, *105*, 1491.

101 G. Steinberg-Yfrach, P. A. Liddell, S.-C. Hung, A. L. Moore, D. Gust, T. A. Moore, *Nature* **1997**, *385*, 239.

102 S. Fukuzumi, *Bull. Chem. Soc. Jpn.* **2006**, *79*, 177.

103 M. Morisue, S. Yamatsu, N. Haruta, Y. Kobuke, *Chem. Eur. J.* **2005**, *11*, 5563.

104 S. Yasutomi, T. Morita, Y. Imanishi, S. Kimura, *Science* **2004**, *304*, 1944.

105 M. R. Wasielewski, *J. Org. Chem.* **2006**, *71*, 5051.

106 J. M. Giaimo, A. V. Gusev, M. R. Wasielewski, *J. Am. Chem. Soc.* **2002**, *124*, 8530.

107 *Supramolecular Dye Chemistry*, *Top. Curr. Chem.*, ed. by F. Würthner, Springer, Berlin, **2005**, Vol. 258.

108 L. L. Miller, K. R. Mann, *Acc. Chem. Res.* **1996**, *29*, 417.

109 H. E. Katz, A. J. Lovinger, J. Johnson, C. Kloc, T. Siegrist, W. Li, Y. Y. Lin, A. Dodabalapur, *Nature* **2000**, *404*, 478.

110 P. Talukdar, G. Bollot, J. Mareda, N. Sakai, S. Matile, *Chem. Eur. J.* **2005**, *11*, 6525.

111 S. Bhosale, S. Matile, *Chirality* **2006**, *18*, 849.

112 N. Sakai, P. Talukdar, S. Matile, *Chirality* **2006**, *18*, 91.

113 N. Sakai, Y. Kamikawa, M. Nishii, T. Matsuoka, T. Kato, S. Matile, *J. Am. Chem. Soc.* **2006**, *128*, 2218.

114 Y. Baudry, D. Pasini, M. Nishihara, N. Sakai, S. Matile, *Chem. Commun.* **2005**, 4798.

115 G. Das, S. Matile, *Chirality* **2001**, *13*, 170.

116 N. Sakai, N. Sordé, S. Matile, *J. Am. Chem. Soc.* **2003**, *125*, 7776.

117 L.-Q. Gu, O. Braha, S. Conlan, S. Cheley, H. Bayley, *Nature* **1999**, *398*, 686.

118 S. Terrettaz, W.-P. Ulrich, R. Guerrini, A. Verdini, H. Vogel, *Angew. Chem., Int. Ed.* **2001**, *40*, 1740.

119 B. A. Cornell, V. L. B. Braach-Maksvytis, L. G. King, P. D. J. Osman, B. Raguse, L. Wieczorek, R. J. Pace, *Nature* **1997**, *387*, 580.

120 J. Cornelissen, M. Fischer, N. Sommerdijk, R. J. M. Nolte, *Science* **1998**, *280*, 1427.

121 D. E. Discher, A. Eisenberg, *Science* **2002**, *297*, 967.

122 A. Mecke, C. Dittrich, W. Meier, *Soft Matter* **2006**, *2*, 751.

Jiri Mareda received Diploma (1975) and Ph.D. (1980) from the University of Geneva for research with Professors C. W. Jefford and U. Burger. He then joined Ken Houks group for a postdoc (1980–1983) before returning to Geneva to focus on computational chemistry in a broad sense.

Naomi Sakai received her B.S. from Keio University (1987) and her Ph.D. from Tokushima Bunri University (1994) for works done at Tokushima Bunri University and Suntory Institute of Bioorganic Research on natural product chemistry. After a postdoctoral stay in the group of Professor Koji Nakanishi at Columbia University (1994–1996), she has been working on the bioorganic chemistry of rigid-rod molecules (Georgetown University, University of Geneva).

Stefan Matile received Diploma (1989) and Ph.D. from the University of Zurich (1994) for research in bioorganic porphyrin chemistry in the group of Professor Wolf Woggon. After a postdoc with Professor Koji Nakanishi at Columbia University on circular dichroism spectroscopy of porphyrins (1994–1996), he developed particular interest in the creation of synthetic multifunctional architecture in lipid bilayer membranes and beyond, first at Georgetown University (1996–1999) and then in Geneva.